GEOPHYSICAL ANALYSIS OF THE ANTARCTIC CONTINENT USING NASA SCATTEROMETER IMAGE DATA

Karen A. Shufeldt

1998

A senior thesis presented in partial fulfillment

of the Bachelor of Science Degree

at the Ohio State University,

Spring, 1998

Advisor:

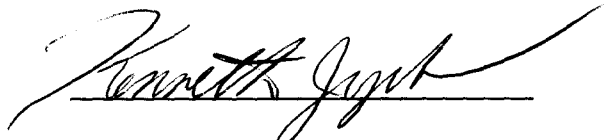

Dr. Kenneth C. Jezek

Abstract

This study involves a quantitative analysis of two maps of the Antarctic continent, one of known bedrock topography, compiled by Drewery and others (1982), and the other comprising NASA Scatterometer data. The objective of this study is to determine if topographic features, indicated on the known bedrock topography map, correspond with those on the map of NASA Scatterometer data. The approach is to draw lineaments on both maps and take strike measurements from a reference point. The orientations of these measurements are compared. A statistical analysis is conducted using rose diagrams, and major measurement trends are taken from these diagrams to be compared between maps. The results include a detailed comparison and discussion of lineaments found on both maps. In general, there is a favorable comparison between both maps suggesting that tonal patterns on the scatterometer data are related to bottom topography. A discussion of lineament trends that correspond to structural features is also included in the results.

TABLE OF CONTENTS

LIST OF FIGURES

Page

1. Introduction

Ice nearly obscures all of the bedrock topography of the continent of Antarctica. The continental ice sheet buries about 98 percent of an area that is larger than the United States and Mexico. This layer of ice and snow is interrupted by only the tallest mountain peaks. Furthermore, the Antarctic terrain cannot be easily mapped because of its vastness and inhospitable climate. As a result scientists use remote sensing methods to map the underlying bedrock topography. Remote sensing is the science and art of obtaining information about an object, area, or phenomenon through the analysis of data acquired by a device that is not in contact with the object, area, or phenomenon under investigation (Lillesand and Kiefer, 1994). For instance, one map used in this study was created using a combination of data produced by Radio Echo Sounding (RES) and Landsat imaging. Aerial photography is also routinely used to give an overall view of the mapping area and to acquire stored data for estimating topography.

This study focuses on two maps, obtained by different methods, of the entire continent of Antarctica. The first map is of the known basal topography of the continent, developed using RES and Landsat imaging. RES relies on the property of high frequency radar waves to penetrate the entire thickness of cold ice sheets. By measuring the time-of-flight of the radar wave through the ice sheet, and assuming a speed of propagation, ice thickness can be estimated to within 10 meters. Basal topography maps are created by differencing surface topography referenced against a standard datum with the ice thickness observation. RES data are acquired either on the surface or from aircraft. Therefore, there are some areas which have been investigated more thoroughly than

others have. For instance, well-studied areas are the ice sheet surrounding the Transantarctic Mountains and the Antarctic Peninsula.

The second map is an image of Antarctica created from NASA Scatterometer data. The NASA Scatterometer is a spaceborne, microwave radar designed to measure wind speed and significant wave height over all of the world's oceans. Data are also acquired over the continents for reserved purposes. Microwave radars only penetrate a few meters into cold snow and ice. The radar wave is sensitive to changes in snow density, grain size, surface roughness, and surface slope. Because ice sheet surface slope is partly controlled by basal topography, there is the possibility that tone variations across NSCAT data can be interpreted as a proxy indicator of subglacial topography. The purpose of this study is to test that hypothesis.

I investigated this hypothesis by studying each map separately and then comparing the results quantitatively, using the RES data as a reference where those data were judged to be of high quality. I first drew lineaments on topographic features of the basal topography map. I then drew lineaments of tonal variations on the map of NASA Scatterometer data. I measured the strike of these lines from the top of the page, corresponding to the 0^{o} meridian. I listed the measurements separately for each map. I then broke the map into sections, comparing the strike measurements using rose diagrams.

This report contains a discussion of the geologic setting of Antarctica, focussing on tectonic aspects and some discussion on the dynamics of the ice sheet. Furthermore, a discussion of the data sets, which comprises the two maps, is provided. The definition of

a lineament, creation of the lineament maps, and analysis by rose diagrams comprises the data analysis portion. Finally, results are provided with conclusions.

2. Geologic Setting

The Antarctic continent covers approximately 14 million square miles, with about 98 percent of its entirety buried under a continental ice sheet. Most of the ice surface lies between 2,000 and 4,000 meters above sea level, and in places the ice sheet can be as much as 4,500 meters thick (C. I. A., 1978). This ice sheet depresses the continent an average of 600 meters. Sea ice annually surrounds the continent.

The breakup of the Gondwana supercontinent, beginning about 177 million years before present, began the formation of the modern Antarctic continent (Webb, 1990). Australia and Antarctica split apart in the Eocene. Southern South America split from the Antarctic Peninsula near the Oligocene-Miocene boundary (1990). From these pieces arose two different sides of one large continent.

Two structurally different sections of Antarctica, East and West, comprise the continent. They are separated by the Transantarctic Mountains, considered as part of East Antarctica. East Antarctica is continental, with a mean crust thickness of 40 km. West Antarctica has a mean crust thickness of 30 km and is an assemblage of continental fragments (Bentley, 1991). The Antarctic Peninsula constitutes part of that complicated assemblage. During the past 60 million years, segments of the Pacific-Phoenix spreading ridge have collided with the western margin of the Antarctic Peninsula from south to north, providing a series of ridge-crest collision episodes (Noltimier et al., 1998).

The geography of East Antarctica includes Queen Maud Land, Wilkes Land, Enderby Land, MacRobertson Land, Coats Land, and Victoria Land. Areas of West Antarctica include the Antarctic Peninsula, consisting of Graham Land and Palmer Land, Ellsworth Land, and Marie Byrd Land. The zone between Graham Land and Palmer Land in the Antarctic Peninsula is termed the Transition Zone. This is defined where the width of the peninsula thins, the curvature changes, and there is significant dissection from glaciers (Noltimier et al., 1998). Well known mountain ranges include the Transantarctic Mountains, the Queen Maud Mountains included within the Transantarctic range, the Ellsworth Mountains (West), the Prince Charles Mountains (East), and the Pensacola Mountains. Notable ice shelves include the Ross Ice Shelf and the Ronne Ice Shelf. Finally, the Weddell Sea and Ross Sea are located on opposite sides of the continent.

2.1 Subglacial Topography

The subglacial topography of East Antarctica contrasts greatly with the topography of West Antarctica. The subglacial crust floor of East Antarctica is largely above sea level, while the subglacial floor of West Antarctica is largely below sea level (Bentley, 1991). In fact, much of the Eastern part of the continent rises a great deal above sea level, as much as 3000 m (the massive Gamburtsev Subglacial Mountains), in the quadrant bounded by the Indian Ocean (the 1st quadrant, defined later in this study) (1991). However, as Bentley points out, in the quadrant nearest to Australia (4thquadrant in this study, defined in the data analysis section), the crust below sea level is separated by highlands (or islands beneath the ice) (1991). In West Antarctica a depression lies

below the Ross Sea and continues below central West Antarctica. The Ellsworth Mountains comprise only one of the few areas that lie above sea level.

2.2 Tectonic Setting

The Jurassic rifting associated with the initial breakup of Gondwanaland relates to the boundary between East and West Antarctica (Bentley, 1991). This is suggested by gravity anomalies found in the Transantarctic Mountains, which mark the boundary. The Transantarctic Mountains are classified as rift-shoulder mountains, characterized by a gently tilted to block-faulted range with a lack of folding or thrust faulting (Stern and ten Brink, 1989). According to Paulsen and Wilson (1998), who used satellite mapping techniques to study the Transantarctic Mountains, the rift zone is comprised of linear to curvilinear fault blocks bounded by a major fault zone along the Transantarctic Mountain front and cut by transverse faults, inferred to lie beneath major outlet glaciers. The average trends (by quadrant from the 0° Meridian) are approximately 345° in the 2nd quadrant, 315° in the 3rd quadrant, and 315°-345° in the 4th quadrant. This information was measured from a map of the continent showing the West Antarctic Rift System and the trend of the rift along the Transantarctic Mountains (Figure 1) (LeMasurier et al., 1991). Furthermore, the Transantarctic Mountains were uplifted approximately 5000 m in 50 million years and have lateral continuity similar to the Andes and Himalayas (Stern and ten Brink, 1989). Flexure of the East Antarctic lithosphere also supports the uplift of the mountains (1989). In fact, flexure controls the subsidence of the Wilkes Basin and Victoria Land Basin, as evidence from topographic and seismic data shows.

The Ross Embayment (Ross Ice Shelf and Ross Sea), Wilkes Basin, and the Antarctic Peninsula all show differing structural integrity. The Ross Embayment is an

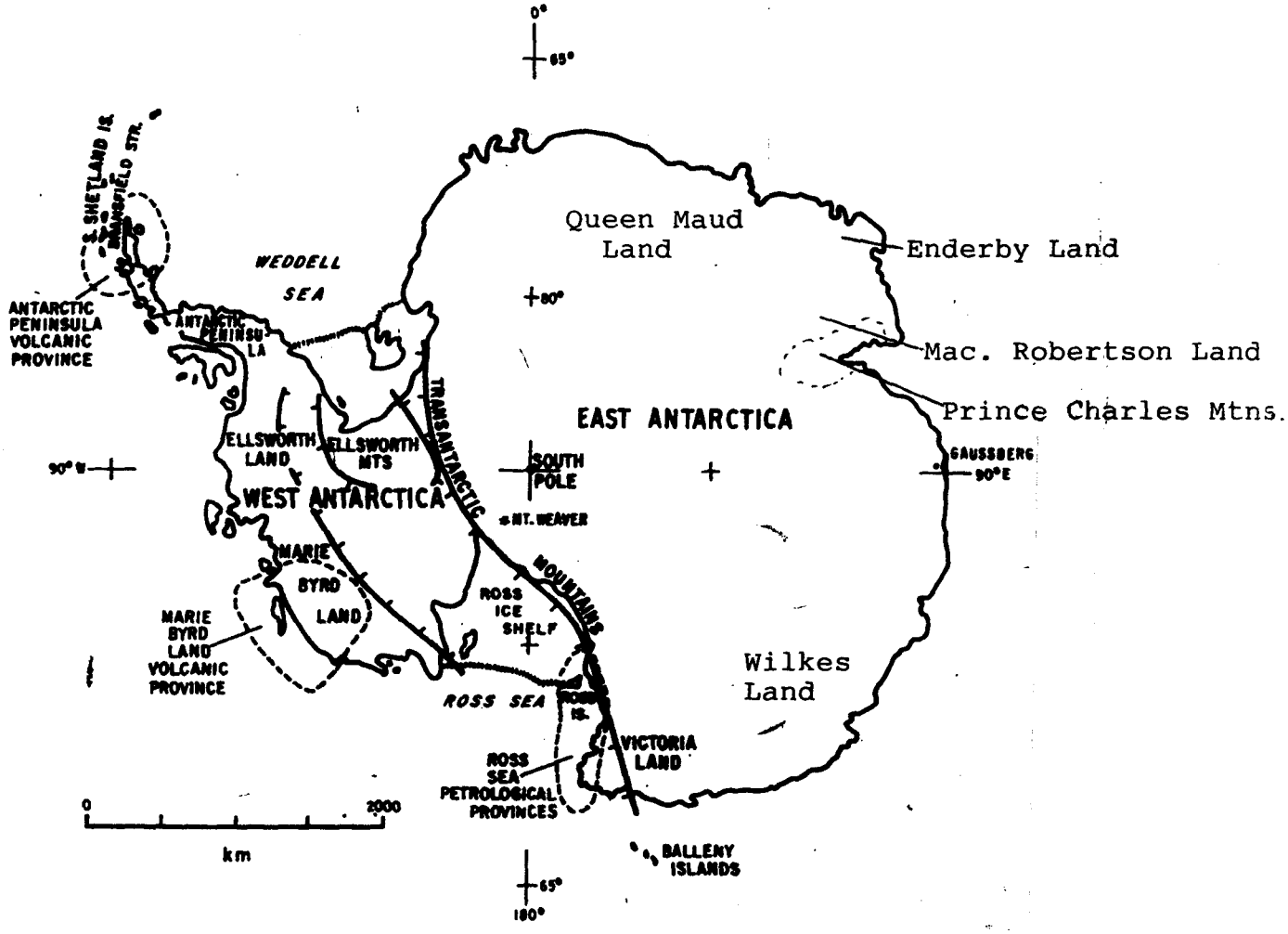

Figure 1: Index map of Antarctica with hachured lines showing an approximation of the West Antarctic rift system. Modified from LeMasurier et al., 1991.

area of active crustal extension between East and West Antarctica (Stern and ten Brink, 1989). It is also characterized by troughs and ridges that are parallel to the Transantarctic Mountains (Bentley, 1991). The Wilkes Basin is covered by at most 3 km of ice, and it runs parallel to the Transantarctic Mountains (Stern and ten Brink, 1989). The basin was produced as a form of regional compensation for the uplift of the Transantarctic Mountains. Volcanic provinces comprise the Antarctic Peninsula (Bentley, 1991). George VI Sound (part of the Antarctic Peninsula) represents a part of a rift system, while another rift system separates the peninsula from the Ellsworth Mountains (1991). Noltimier (1998) has done lineament analysis on structural features such as fault, dyke, bedding, and rock cleavage trends. Major trends from this study, measured from True North, include a major dyke trend at 330°–360° (corresponding to a trend from Grid North of approximately 300°-330°), a lesser dyke trend between 270° and 290° (10°– 30° from Grid North) a major fault trend from 350°–360° (320°-330° from GN), and a lesser fault trend between 290° and 300° (between 260° and 270° from GN).

2.3 The Continental Ice Sheet

Antarctica contains an area of 13.6 x 10^6 square kilometers that is covered by 30 x 10^6 cubic kilometers of ice (Denton et al., 1991). The West Antarctic Ice Sheet is marine because the bedrock floor on which it sits would remain under water if the ice were removed, accounting for isostatic rebound (1991). It has measurable topographic features, such as divides, domes, and saddles of low elevation (1991). The East Antarctic Ice Sheet is larger than the West and is terrestrial, because it rests on a base is predominantly above sea level (1991). It is also characterized by complex and variable surface topography.

Ice shelves (floating slabs of glacier ice) and sea ice also fringe the Antarctic continent. The most notable ice shelves are the Ross Ice Shelf and Ronne Ice Shelf (both mentioned previously). Sea ice covers 20 x 10^6 square kilometers in the winter and 4 x 10^6 square kilometers of ocean in the summer (Denton et al., 1991). It forms near the continent in the autumn and spreads outward throughout the winter (1991).

3. Data Sets

3.1 Basal Topography

The initial data set, which constitutes a basal topographic map of the Antarctic continent, is taken from a map of the bedrock configuration compiled by D. J. Drewry and others, published as part of an Antarctic glaciological and geophysical folio by the Scott Polar Research Institute (SPRI) in 1982. It was made available in digital format for this project. The information in the SPRI folio also includes data on Antarctic ice-sheet surface morphology and ice thickness. The following information on this data set is taken from Drewry et al., 1982.

The data were primarily obtained from airborne Radio Echo-Sounding (RES). Accurate surface and subglacial elevations are achieved using 60 MHz radar sounding data and aircraft navigation data. The initial sources include altitude control, recorded altitude, RES films, navigation control, and navigation data, which were all adjusted and reduced to produce final elevation data. Furthermore, improvements in the mapping of the Antarctic coastline are due to the use of Landsat images fixed to geodetic ground control. RES and all other available data on subglacial topography have been combined and contoured [in the SPRI folio] (Drewry et al., 1982).

The map of bedrock configuration in the SPRI folio contains areas of high data coverage (Grid South) and lower (relative) data coverage (Grid North). The areas of high data coverage show a contour interval of 250 m. Elsewhere the contour interval is 500 m. Drewry and others used histograms of RES-derived bedrock elevations in East, West, and for all Antarctica covered by RES grid (which is approximately 50% of the continent). He noted that East Antarctica has the more normal (Gaussian) distribution of elevations compared with West Antarctica. This is probably accounted for by failure of the RES system to detect deep bedrock in the vicinity of the Bentley Subglacial Trough and parts of the Byrd Subglacial Basin. Ice thicknesses here are in excess of 4 km and two-way dielectric absorption is high as a result of warmer ice temperatures (Drewry et al., 1982). Figure 2 shows the initial, digital bedrock topography image of Antarctica used in this study.

3.2 NASA Scatterometer Data

The NASA Scatterometer (NSCAT) is a calibrated microwave radar, and can penetrate the atmosphere under virtually all conditions, (Lillesand et al., 1994). NSCAT operates at an approximate frequency of 14 GHz, corresponding to a wavelength in air of approximately 30 cm. Microwaves have a wavelength out to 30 cm. NSCAT was launched in August, 1996 aboard the Japanese Advanced Earth Observing System (ADEOS-I) and operated for 9 months, providing wind observations of unprecedented coverage, frequency and accuracy which were used in weather forecasting, climate modeling, and air/sea interaction studies (Drinkwater and Long, 1997). Drinkwater and Long (1997) have generated a time series of radar images of the Antarctic region using the Scatterometer Image Reconstruction with Filtering (SIRF) resolution enhancement

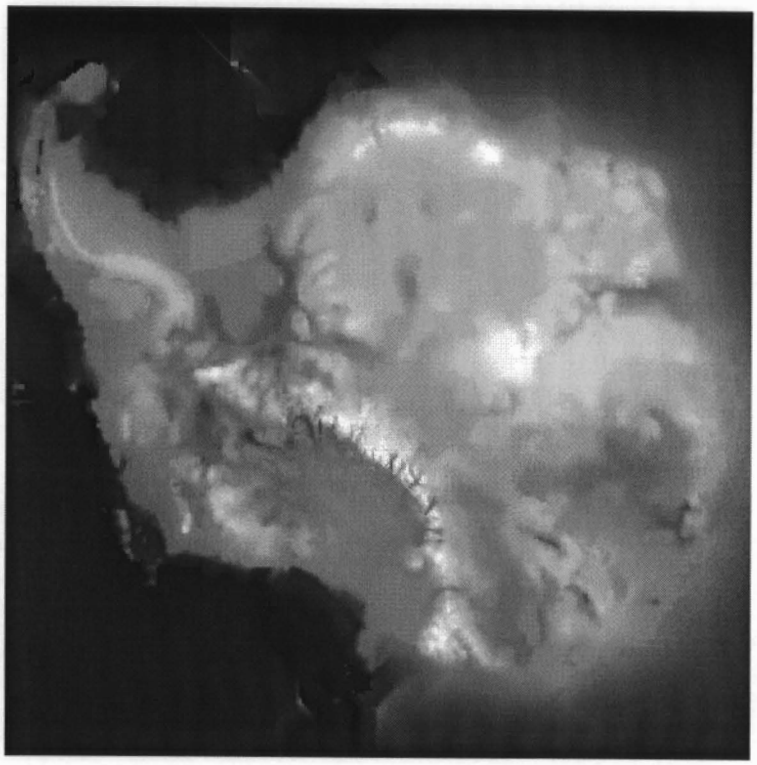

Figure 2: Digital bedrock topography image of Antarctica (Drewry et al.,1982)

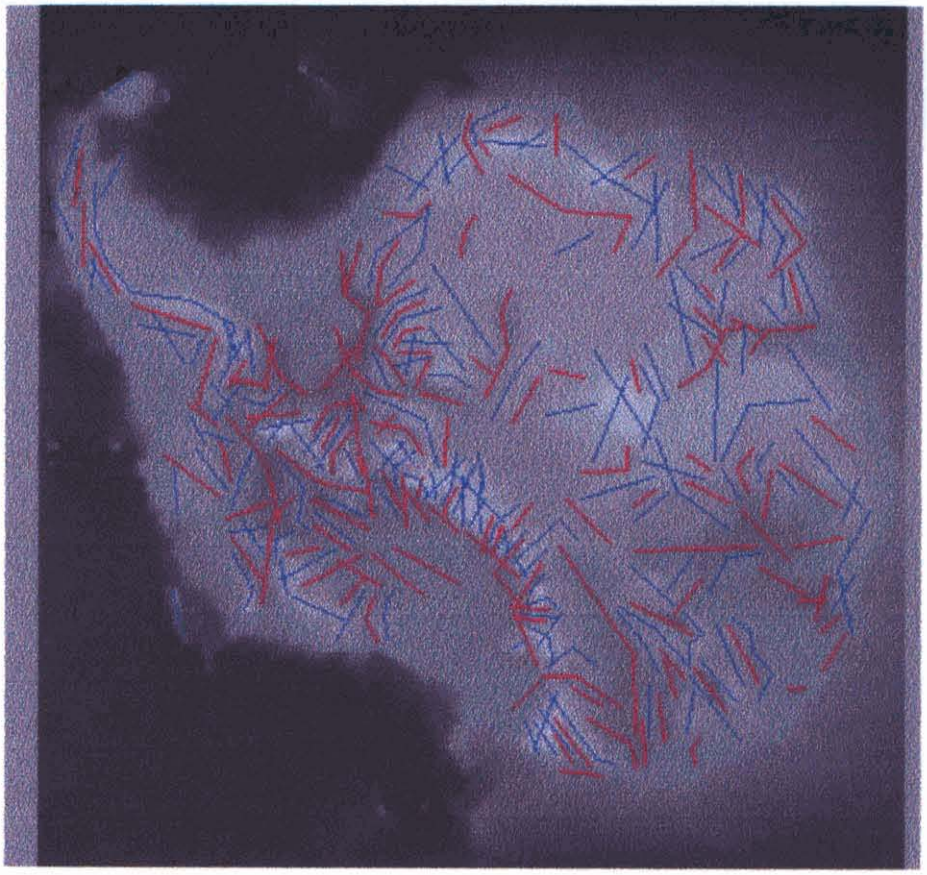

Figure 3: Digital bedrock topography image of Antarctica (Drewry et al., 1982) showing lineaments

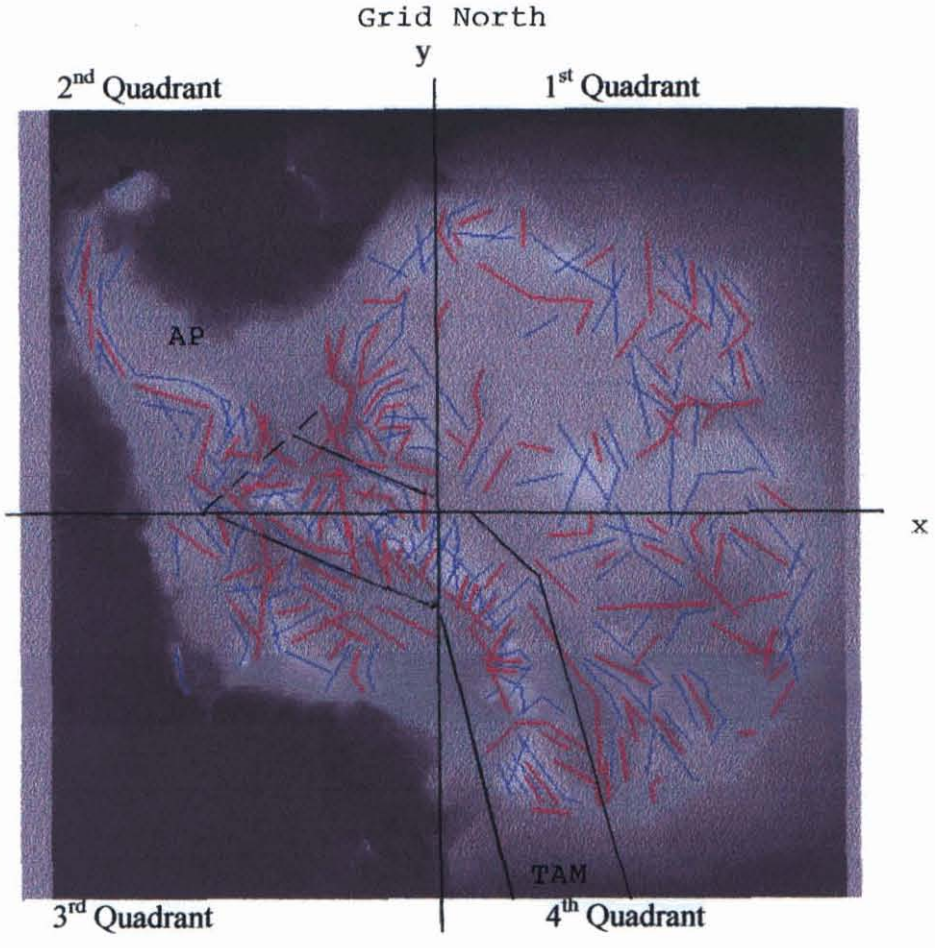

AP--Antarctic Peninsula
TAM--Transantarctic Mountains

Figure 4: Digital bedrock topography image of Antarctica (Drewry et al., 1982) showing lineaments and section/quadrant divisions

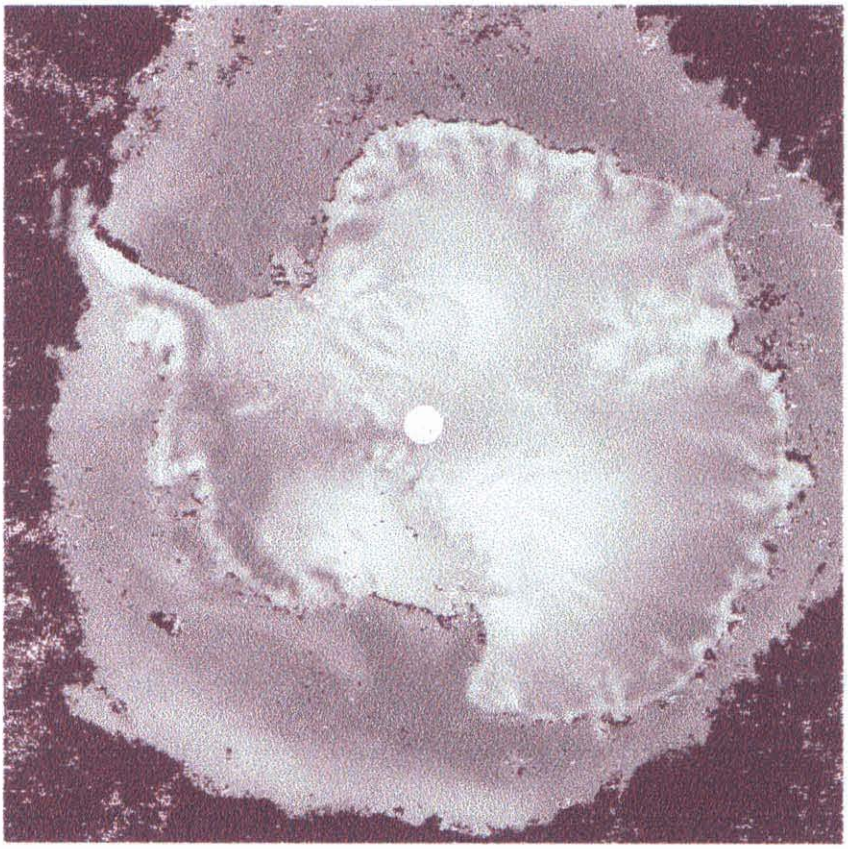

Figure 5: Digital map of NASA Scatterometer (NSCAT) data

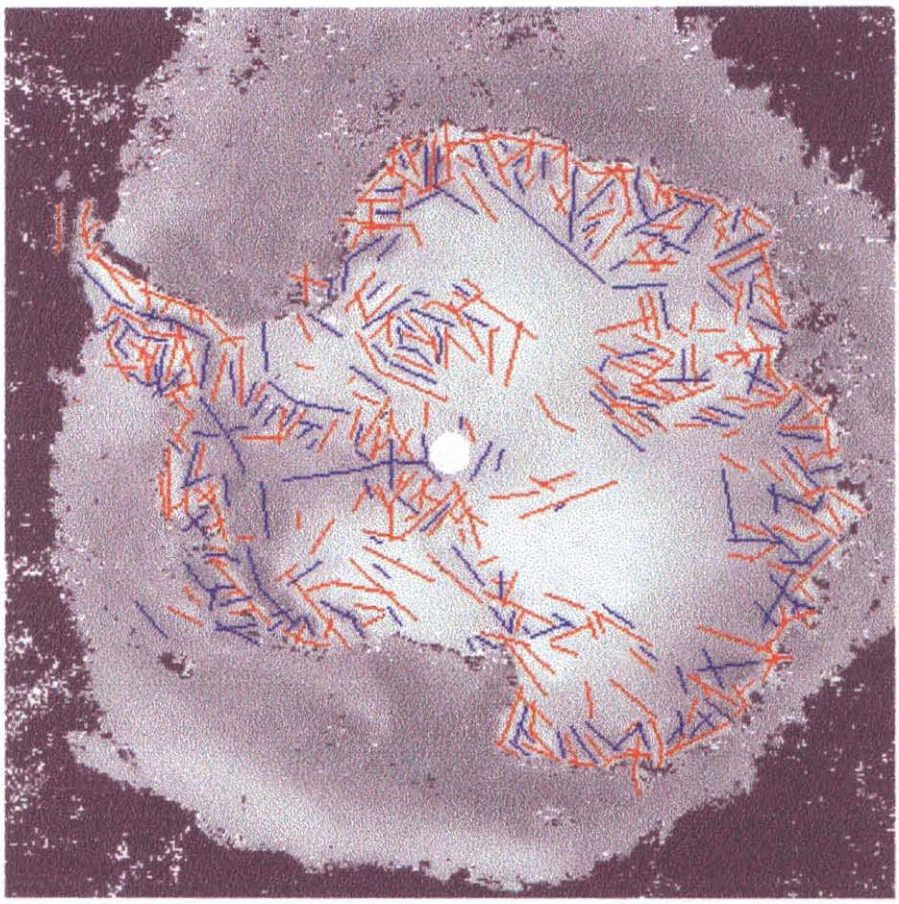

Figure 6: Digital NSCAT image showing lineaments

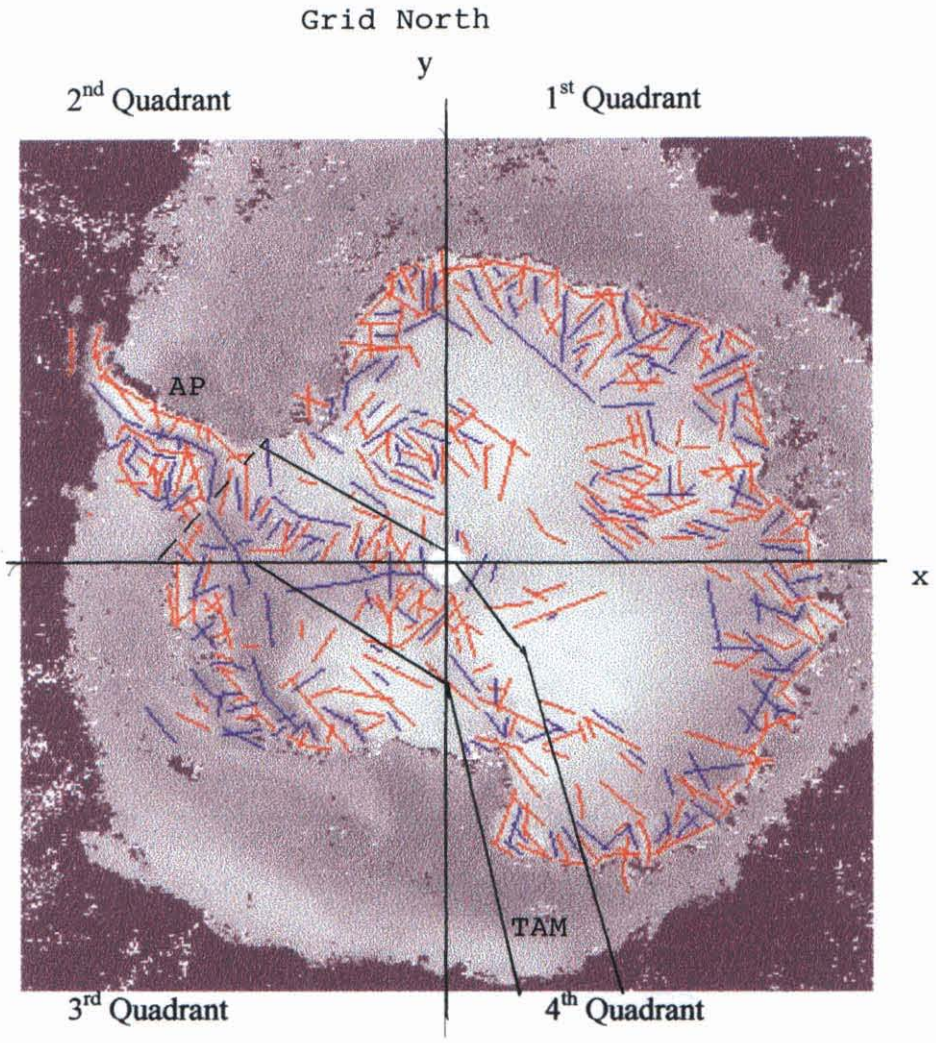

AP--Antarctic Peninsula
TAM--Transantarctic Mountains

Figure 7: Digital NSCAT image showing lineaments and sections/quadrants

algorithm and discuss the use of NSCAT in relation to this algorithm to further study Antarctica. The digital map of Antarctica (figure 5) used in this study was generated using NASA Scatterometer data (Kwok, 1997).

The scatterometer produces rapid coverage and frequent generation of global images. The microwave images depend on both surface roughness and the electrical properties, which vary for different ice types. NSCAT makes measurements at both vertical and horizontal electrical polarization at a variety of azimuth angles and can observe the ice from a variety of incidence angles, further enhancing the utility of the radar data (Drinkwater and Long, 1997). The size of the resolution cell used in this study is 50 square kilometers.

4. Data Analysis

4.1 Lineament Definition

This study incorporates lineament analysis to interpret the basal topography and NASA Scatterometer maps of Antarctica. That is, lineaments are drawn on the two figures. The lineaments represent topography on the RES map and represent variations in radar backscatter on the NSCAT map. The general definition of a lineament is simply expressed using the parameters of the maps themselves. In each case, a lineament represents a linear, elongate feature on a map. For this study it must be at least 20 kilometers in length. It is denoted by ridges, valleys, gullies, elongate islands, and peninsulas. In the case of the NSCAT data, it could also represent changes in the properties of the glacier surface on the bedrock topography map. The lighter features are higher in elevation and the darker features are lower. I came to this conclusion after

comparing the original bedrock topography map, depicted in color, from Drewry and others to the computer generated map in grayscale from the same source. The hard color copy of the map has labeled elevations and can be roughly compared with the unlabeled digital map. The Scatterometer data only show variations in radar backscatter strength, which as noted earlier, may have several causes.

4.2 Bedrock Topography Map

Using ERDAS Imagine, I drew the lineaments on the distinguishable features on the bedrock topography map. Figure 2 shows just the digital map of the bedrock topography without lineaments. For ease in measuring, the features with relatively high elevations (light gray to white on the map) are drawn in red, while the low lying areas (gray to dark gray on the map) are drawn in blue. Figure 3 shows the map with lineaments. In the statistical analysis, the different elevations were not considered, and the rose diagrams were created, separating the data only by geography. I then separated the map into sections based on a rough quadrant system. There are four quadrants, numbered counter clockwise from upper right of page. These quadrants split the continent into nearly equal divisions. When analyzing the data, I also separated the Transantarctic Mountains, plus the Antarctic Peninsula into a category and the Antarctic Peninsula alone into another. However, each quadrant (1 through 4) contains part of the Transantarctic Mountains and/or the Antarctic Peninsula. Figure 4 shows these divisions.

4.3 Map of NASA Scatterometer Data

The lineament map for the Scatterometer data was created in a similar fashion to the map showing bedrock topography. I again used ERDAS Imagine to display the map and the lineaments. Figure 5 shows only the NSCAT map without lineaments. I drew

red lineaments on features I deemed to be relatively high elevations and blue lineaments on relatively low features. The same criteria were used. At this time I had not compared the two maps in order to stay as objective as possible when drawing the lineaments. Figure 6 shows the initial map with lineaments. I split this map into four quadrants similar to the bedrock map. Each quadrant contains nearly the same area as the corresponding one on the bedrock topography map, owing to some human error. I used the Transantarctic Mountains, plus the Antarctic Peninsula in one category again and the Antarctic Peninsula alone in another. Figure 7 shows the divisions of the map.

4.4 Rose Diagrams of Strikes

Rose diagrams are used to complete a statistical analysis of the lineaments derived from the two data sets.

Since the maps are split into sections and quadrants, I divided the measurements the same way in order to compare them later. I measured the strike of each line from the Prime Meridian on a coordinate map. Consequently, the strikes are measured relative to the Grid system adapted for aerial navigation maps of the Antarctic. In this system Grid North is up. The strike measurement is the degree measurement clockwise from the line of the Prime Meridian, or top of page. (See axis marked "y" on figures 4 and 7). To keep the data succinct, I measured the strikes from 0 to 90 degrees and 270 to 360/0 degrees, ignoring the lower (southern) portions of the grid. For example a strike of 45 degrees corresponds to a strike of 225 degrees, but on the diagram the 45-degree measurement is used. I also divided the measurements by color but later combined these (by section) for analysis.

Rose diagrams are statistical representations of numerical data in degrees. They show the number of measurements and orientation of those measurements divided into a certain bin size. The larger rays that radiate from the origin (center) represent a higher number of measurements. I used Matlab to create these diagrams, and the bin size used was 18 degrees. I created a total of twelve rose diagrams (see Appendix A), six for the known bedrock topography (figures A1, a-f), and six for the Scatterometer data (figures A2, a-f). The comparative sections comprise the Transantarctic Mountains plus the Antarctic Peninsula (figures A1a and A2a), the Antarctic Peninsula by itself (figures A1b and A2b), the 1st quadrant (figures A1c and A2c), the 2nd quadrant (figures A1d and A2d), the 3rd quadrant (figures A1e and A2e), and the 4th quadrant (figures A1f and A2f). Using this breakdown, I can compare the respective sections.

4.5 Analysis of Rose Diagrams and Major Trends Per Section

The rose diagrams show clear strike trends, denoted by large (relative) numbers of measurements, for each section. These trends are observed with the unaided eye on both maps. The trends themselves are the focus of the analysis, while the frequency (number of measurements per average trend divided by the total number of measurements multiplied by 100 for a percent) is used primarily to choose the dominant trends. The frequency is also used as a basic ranking system when comparing each section. This will be evident in the coming discussion. I chose three dominant trends per diagram for comparison. I organized my results in table 1, which shows the angle in degrees of the average orientation and the frequency (a percent, as defined above) of each orientation.

Table 1: Major Lineament Trends on the Bedrock Topography Map and Map of Scatterometer Data

Map Area	*	Bedrock Topography		Scatterometer		Comparison
		trend	occurrence	trend	occurrence	
Transantarctic Mountains (+AP)	a	26	17%	26	21%	very good
	b	315	16%	315	17%	(best)
	c	45	16%	10	15%	
Antarctic Peninsula	a	26	19%	27	23%	very good
	b	334	19%	10	20%	(2nd)
	c	278	19%	280	14%	
1st Quarter	a	26	26%	296	15%	moderate
	b	333	13%	45	14%	(worst)
	c	316	11%	317	14%	
2nd Quarter	a	25	18%	11	17%	good
	b	11	13%	27	14%	(3rd)
	c	334 & 278	13%	45 & 297	11%	
3rd Quarter	a	351	17%	315	16%	good-mod.
	b	315	16%	45	14%	(4th)
	c	27	14%	82 & 350	11%	
4th Quarter	a	315	22%	317	23%	moderate
	b	28	13%	297	14%	(5th)
	c	47	13%	333	10%	

Measurements are in degrees, and are the median of the rose range for that type
*a, b, and c denote frequency of average measurement (I.e. "a" is most frequent)

Overall, the major trends of orientations correlate between Drewry's known bedrock topography map and the map of NASA Scatterometer data according to table 1. The measurements for the Transantarctic Mountains (TAM) have the best correlation of the six sections studied on each map. (Again, see figures 4 and 7 for section and quadrant divisions.) According to Paulsen and Wilson (1998), large linear features shown on the

satellite imagery denote structural weaknesses, which are caused by preferential erosion along faults and fractures that creates topographic depressions exploited by glacial drainage systems. Of the three TAM trends, strikes at 315° and 26° compare favorably. The next most dominant trends extracted from the two maps do not compare. Possibly glacial features are being represented on the NSCAT map, which, of course, do not show on the bedrock topography map, giving an alternate trend.

Another area, which has much information available, is the Antarctic Peninsula (AP). It also shows favorable comparison between the two maps; but it is not as good as the comparison for the entire extent of the Transantarctic Mountains. There is also a major trend for the Antarctic Peninsula of 26 degrees for the bedrock topography map and 27 degrees for the NSCAT map. This matches the same trend for the Transantarctic Mountains because the AP is included in the rose diagram for the TAM. Another favorable comparison for the rose diagrams of the AP is the one that shows the orientation of 278 degrees for the bedrock topography and 280 degrees for the NSCAT map. This analysis of the AP is also corroborated by a recent study from Noltimier et al. (1998). In that study similar overall NE (corresponding to 26/27 degrees) and NW (corresponding to 278/280 degrees) trends are shown on a rose diagram which incorporates more data from SAR lineament mapping. Lineaments were drawn on SAR data, and most represent the lesser dyke and fault trends.

The 1st quadrant of the maps, according to the rose diagrams, shows the worst comparison. It also has the poorest quality RES data. It still shows one trend of good correlation, 316 degrees basal topography and 317 degrees NSCAT, however. These are not the largest trends, however, and the others do not relate.

The 2nd quadrant shows favorable comparison between the two maps with one trend at 25 degrees (bedrock) and 27 degrees (NSCAT) and another major orientation at 11 degrees for both. The other trends are off by at least 19 degrees for quadrant two.

The 3rd quadrant displays moderate comparison, having two trends relate. These include 315 degrees for both and 351 degrees (basal) and 350 degrees (NSCAT). However, these correlating orientations have very different frequencies, and the other instances do not match.

Finally, the 4th quadrant has moderate comparison with one good match at 315 degrees (bedrock) and 317 degrees (NSCAT). These are both the most frequent major orientations. The other trends, however, seem to be opposites, and therefore are not good indicators of favorable comparison. Because the major trends of each section match to at least some extent and usually match very well, the hypothesis of this study has been verified. In other words, I find that the two maps, the map of known bedrock topography and the map of NASA Scatterometer data, correlate and conclusions can be made from this fact.

5. Results.

5.1 Data Relation to Structure

The dominant trends for the Transantarctic Mountains on both maps show the best correlation, as outlined in the data analysis section. To recap, the major orientations are trending 26 degrees and 315 degrees. These lineaments define the topographic features on both maps that are related to the uplift (extension) of the crust in the Transantarctic Mountains. According to Paulsen and Wilson (1998), large linear features shown on the

satellite imagery denote structural weaknesses, which are caused by preferential erosion along faults and fractures that creates topographic depressions exploited by glacial drainage systems. The longer relative trends seem to be oriented more towards 26 degrees, while the shorter lineaments, which intersect these longer lineaments (in general "cross" patterns), are comprised of mostly the 315-degree trends. Generally, these measurements reflect the major rift associated with the TAM (denoted by trends approximately 315 degrees) and the glacial drainage systems caused by preferential erosion (denoted by trends approximately 26 degrees) (Paulsen et al., 1998). This is not always the case, but when comparing just those two major orientations, it is a prominent observation.

On the Antarctic Peninsula (alone) the lineaments are few, but easily seen. They seem to mark the rift associated with George VI Sound and the trend of the features on the rift between the AP and Ellsworth Mountains. This shows on both maps. The comparison between the two maps, as mentioned previously, is very good, second only to the favorable comparison of the Transantarctic Mountains. The major trends are 26/27 degrees and 278/280 degrees. The rift features for George VI Sound correspond to the 278/280-degree major orientations, while the features that mark the rift separating the AP from the Ellsworth Mountains correspond to the trend of 26/27 degrees. In Noltimier's study (1998) trends between 270° and 290° correspond to a lesser clustering of fault trends. The trends of the more major clustering of dyke trends lies between 300° and 330° (measured from Grid North). There is another lesser trend of 10 –30 degrees, representing dykes (1998). These are general observations.

The coastal areas also have numerous lineaments represented on both maps. However, because of the quadrant divisions used in this study, it is rather difficult to do a quantitative study on just the coast of the Eastern part of Antarctica. In fact, East Antarctica, which corresponds to the 1st and 3rd quadrants shown in figures 3 and 6, contains major lineament trends with the worst correlation found in this study. The 1st quadrant has the worst correlation, while the 3rd quadrant is fourth. The fact remains, however, that these areas are not studied as frequently as areas west. Perhaps the NASA Scatterometer data shows a better representation of the continent in these areas than Drewry's map of bedrock topography.

The Ross Embayment represents a well-known area with poor topographic expression. This is because it is made up of the Ross Sea and the Ross Ice Shelf. Features are located below sea level and are not shown on either map. Only some depressions or low lying (relative to surrounding areas) features have representative lineaments.

5.2 Overall Lineament Trend and Map Comparison

As stated previously, the map of Scatterometer data correlates well with the map of known bedrock topography. This is the overall conclusion. Geographic areas of the continent, which seem to have representative trends on both maps, include the Transantarctic Mountains, the Antarctic Peninsula, Victoria Land, Ellsworh Land, and the Ellsworth Mountains. On both maps in the Eastern coastal areas, numerous lineaments are drawn. On both maps the inland areas of East Antarctica have a lack of lineaments, possibly due to the thick terrestrial ice sheet which covers that area. It tends to be

featureless because the underlying bedrock is cratonic and not marked by distinct structural features, as stated previously (Bentley, 1991).

Exceptions to the favorable correlation between the two maps are also found in East Antarctica, in the areas of Wilkes Land, MacRobertson Land and Queen Maud Land. In general, more lineaments are found on the map of Scatterometer data. This means that there is more possible information contained in the NSCAT map than on the map of bedrock topography. Wilkes Land is an exception in that the map of basal topography has an area covered with spaced lineaments, while the NSCAT map does not contain any for that region.

Aside from simple human error, two possibilities arise for the absence or presence of lineaments on either map. First, NSCAT lineaments could be drawn on surface glacial features, which are not represented in the underlying bedrock topography. Grounding lines, ice streams, or flow divides may be represented in the NSCAT data but do not necessarily correlate with basal topography. The second possibility concerns the accuracy of Drewry's known bedrock topography map compared to the map of NASA Scatterometer data. Simply, more information may be available using the Scatterometer. The numerous lineaments shown in East Antarctica, an area not mapped frequently by conventional methods, may have features accurately represented by the NSCAT map.

Two of the extra features seen on the map of NASA Scatterometer data that are not represented in Drewry's data set are located in East Antarctica. There is a feature with lineaments oriented in an almost circular pattern found in Queen Maud Land (near Coats Land next to the Ronne Ice Shelf). Most of this feature is included in the 1st quadrant and the rest is located in the second quadrant. It does not seem to be related at

all to the Transantarctic Mountains. Perhaps this is one reason the 1st quadrant did not correlate as well between maps as the other sections/quadrants. The second feature looks to be a continuation of the Prince Charles Mountains, located in MacRobertson Land, on the NSCAT map. This is also the 1st quadrant. More lineament detail (dense lineaments) can be seen on the map. This may better represent the Prince Charles Mountains, compared to the bedrock topography map.

5.3 Analysis of Summary Table of Lineament Trends

Table 2 is a rearrangement of table 1 to highlight comparisons between strike trends measured on both maps. One observation is that strikes at 26/27 degrees and 315 degrees occur in almost every data set. This may be a consequence of the measurement technique. For each bin (measured 18 degrees), I drew a median line to show the average for that bin. The degree measurements, 27 and 315 are simply representations of the median of a bin. Since the bin size is large (18 degrees), the analysis is probably masking local variability. Another possible reason for this phenomenon is due to geography. Each section and quadrant contains part of the Transantarctic Mountains and/or the Antarctic Peninsula, which are both dominated by the 27- and 315-degree trends.

Table 2: Summary of Major Lineament Trends on the Bedrock Topography Map and Map of Scatterometer Data

Map Area	Bedrock Topography	Scatterometer
	trend	trend
Transantarctic Mountains (+AP)	26	26
	45	10
	315	315
Antarctic Peninsula	26	10
	278	27
	334	280
1st Quarter	26	45
	333	296
	316	317
2nd Quarter	11	11
	25	27
	334 & 278	45 & 297
3rd Quarter	27	45
	315	315
	351	82 & 350
4th Quarter	28	297
	47	317
	315	333

Measurements are in degrees, and are the median of the rose range for that type.
This is a rearrangement by measurement size of table 1

6. Conclusions

Lineaments represent structural features on two separate maps of the Antarctic continent, one a data set taken from the SPRI folio of the known bedrock topography compiled by Drewry and others, and the other a map of NASA Scatterometer data. Upon comparison of these lineament trends, the major orientations of the lineaments, broken

into sections for comparison, correlate between the two maps. This leads to the conclusion that the map of NASA Scatterometer data presents a satisfactory representation of the underlying bedrock topography of Antarctica. Based on this fact, the structural orientation of the bedrock for vaguely mapped or explored areas of the Antarctic continent (especially in the eastern part of the continent) can be preliminarily inferred using the NASA Scatterometer data.

6.1 Possible Explanation for Unknown Features

The two notable features mentioned in the results section include the circular feature in Queen Maud Land and the extension of the Prince Charles Mountains in MacRobertson Land. The circular feature is not so easily explained due to the cratonic nature of East Antarctica in that area. However, this feature may be near enough to the Theron Mountains and even the Transantarctic Mountains to be thought to have experienced some sort of uplift. The major trends, however, do not seem to match with the major orientations (table 1) found for the Transantarctic Mountains. Many trends for the feature are nearly 0 degrees. Also the circular nature itself is puzzling. The data for this feature taken in this study is, therefore, inconclusive. The other feature is probably just the Prince Charles Mountains better represented with the NSCAT data.

6.2 Error Analysis and Limitations

Four cases of human error need to be considered in this study. First, the map resolution can distort the features on the map causing problems when physically drawing the lineaments. Second, some measurements could have been missed or counted twice. This could happen again in the data entry of the measurements for creation of the rose diagrams. However, since there are so many total measurements (near 800), this is

probably negligible. Third, there is an initial measurement error of +-5 degrees on the lineaments, which were measured by hand. Finally, after creating the rose diagrams, I estimated each major trend. There is a possible error there of up to 5 degrees. Therefore, for table 1 the highest possible error in degree measurements is +-10 degrees.

In addition to human error, basic project limitations need to be considered. First, if the resolution of the maps was better, more accurate measurements could possibly be made. Also, as previously stated, glacial features may easily be confused with underlying bedrock topography features. This is more likely to be seen in areas like West Antarctica due to its rugged bedrock topography, which may cause furrows, domes, or divides in the overlying ice (Denton, 1991). This is a very real possibility for this project as speculated previously in the results section. Other tools, such as Digital Elevation Models (DEMs) can possibly be used to more accurately represent such features.

6.3 Possibilities for Related Future Projects

The accuracy of this study can be greatly increased in a number of ways. First, if the areas of interest were broken down into smaller portions, a more detailed survey can be conducted. For instance, each lineament could be numbered and placed in a database. Furthermore, the best way to increase the accuracy would be to reference the features somehow, as with a coordinate system. This way, an exact location for each feature can be stored for one map and then compared to the corresponding feature (area) on the other map. Each measurement orientation could be compared in this way. Also, more research on the new features on the map of NASA Scatterometer data can be conducted. This

on the new features on the map of NASA Scatterometer data can be conducted. This would include the origin of such a feature and a possible history. There was not enough time in this project to explore any of these possibilities thoroughly.

7. Acknowledgements

This work was completed using NASA Scatterometer data provided by Dr. Ronald Kwok of NASA's Jet Propulsion Laboratory.

I would also like to thank Dr. Kenneth Jezek for his support and resources on this project.

9. References

Bentley, Charles R., Configuration and structure of the subglacial crust, in The Geology of Antarctica, ed. Robert J. Tingey, Clarendon Press, Oxford, 1991, pp. 335-364.

C. I. A., Polar Regions Atlas, GC 78-10040, 1978, 66 pp.

Denton, George H., Michael L. Prentice, and Lloyd H. Burckle, Cainozoic history of the Antarctic ice sheet, in The Geology of Antarctica, ed. Robert J. Tingey, Clarendon Press, Oxford, 1991, pp. 365-433.

Drewry, D. J., S. R. Jordan, and E. Jankowski, Measured Properties of the Antarctic Ice Sheet: Surface Configuration, Ice Thickness, Volume and Bedrock Characteristics, *Annals of Glaciology, 3,* 1982, 10 pp.

Drinkwater, Mark R. and David G. Long, Antarctic Applications of Scatterometer Image Data, unpublished manuscript, 1997.

Kwok, R, NASA Scatterometer personal communication, 1997.

LeMasurier, Wesley E. and D. C. Rex, The Marie Byrd Land volcanic province and its relation to the Cainozoic West Antarctic rift system, in The Geology of Antarctica, ed. Robert J. Tingey, Clarendon Press, Oxford, 1991, pp. 249-284.

Lillesand, Thomas M. and Ralph W. Kiefer, Remote Sensing and Image Interpretation, 3rd ed., John Wiley & Sons, Inc., New York, 1994, 750 pp.

Noltimier, Katy F., Kenneth C. Jezek, Terry J. Wilson, Evidence for the Tectonic Segmentation of the Antarctic Peninsula from Integrated ERS-1 SAR Mosaic and Aeromagnetic Anomaly Data, BPRC Technical Report 98-02, 1998, pp. 19-22.

Paulsen, Timothy and Terry J. Wilson, Declassified Satellite Photos Provide First Views of Southern Transantarctic Mountains, *EOS*, 79, 8, February 24, 1998.

Stern, Tim A. and Uri S. ten Brink, Flexural Uplift of the Transantarctic Mountains, *J. of Geophysical Research*, 94, B8, 1989, pp. 10,315-10,330.

Webb, Peter-Noel, The Cenozoic history of Antarctica and its global impact, *Antarctic Science,* 2, 1, 1990, pp. 3-21.

APPENDIX A:

Section 1: Rose diagrams for Drewry's known bedrock topography map

Figures a-f, referenced in text as A1 (a-f)

Section 2: Rose diagrams for the map of NASA Scatterometer data

Figures a-f, referenced in text as A2 (a-f)

Section 1: Bedrock topography

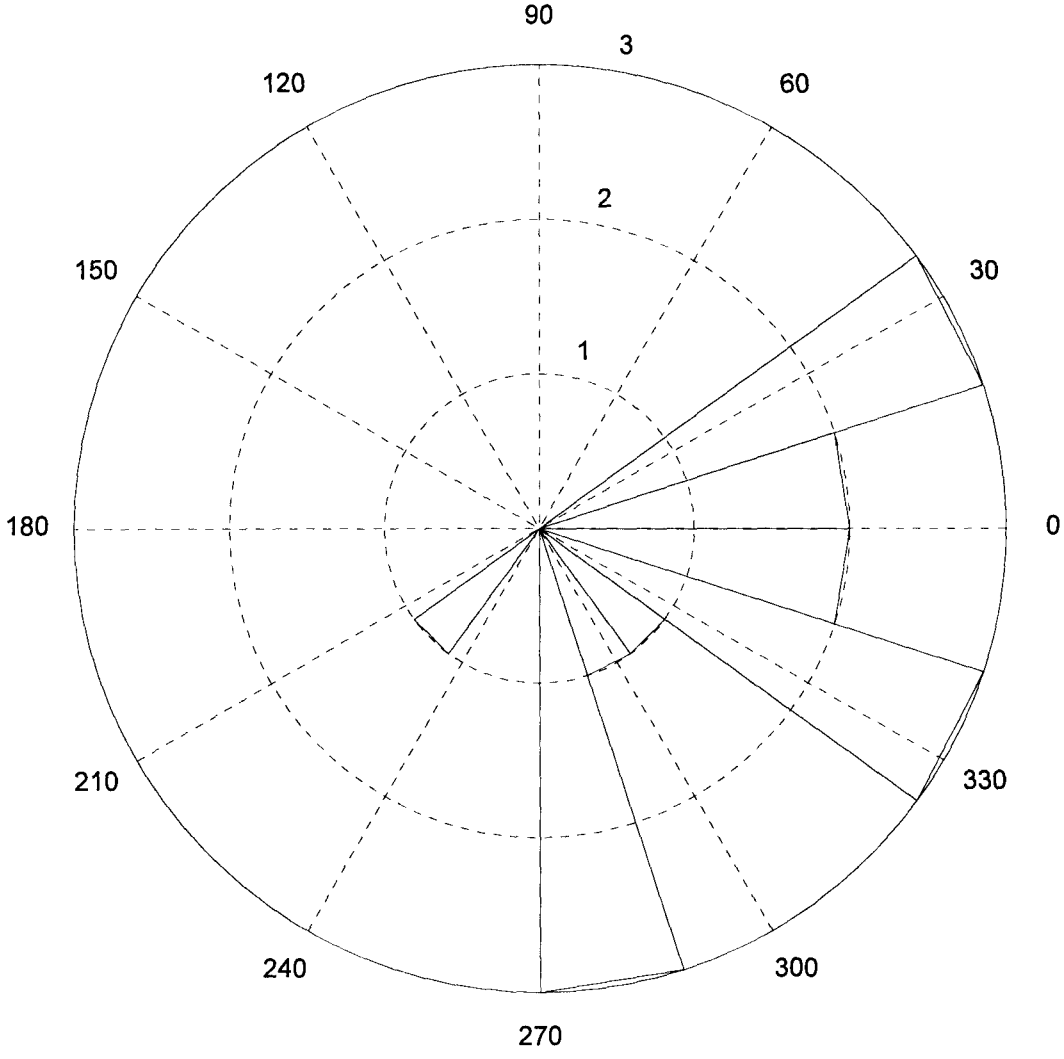

Figure a: Antarctic Peninsula

Section 1: Bedrock topography

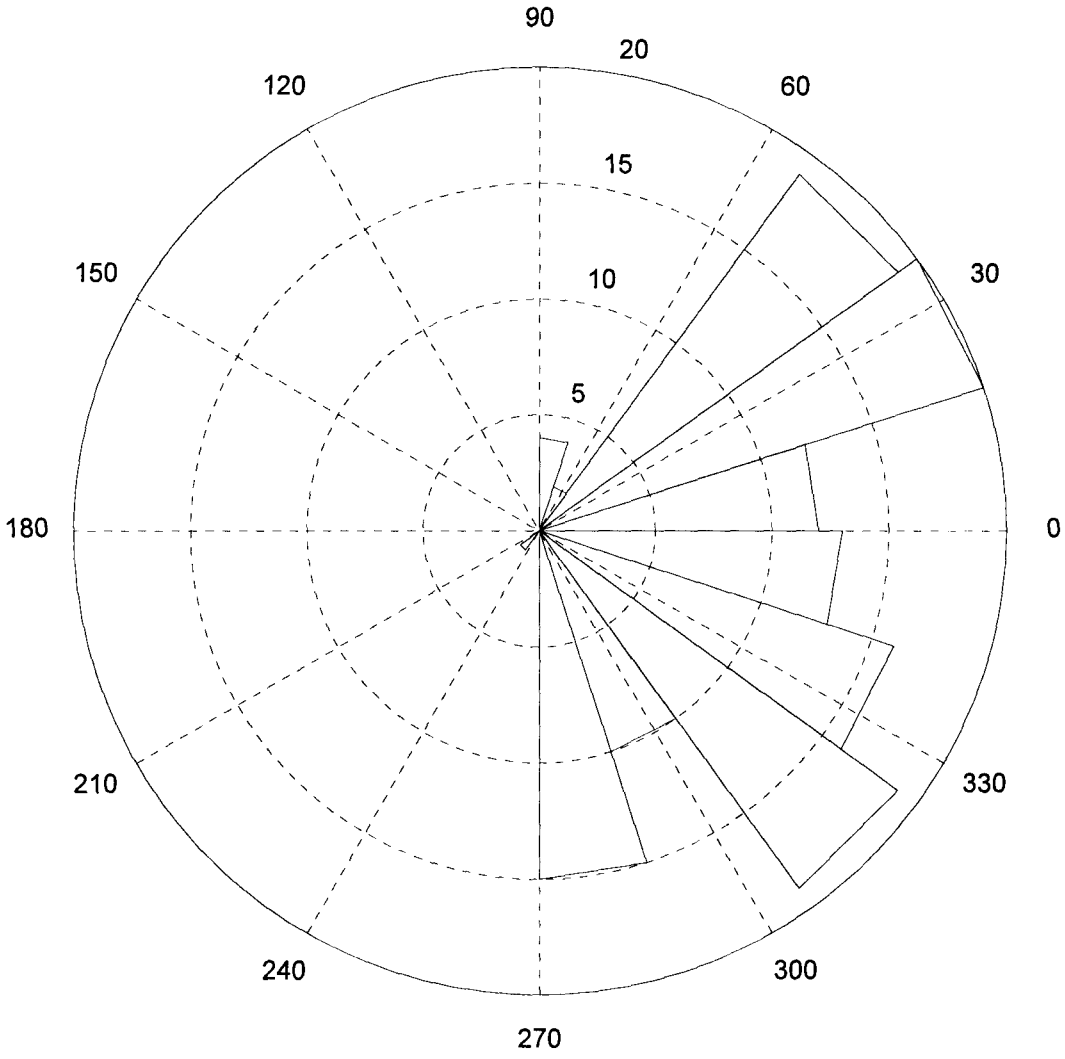

Figure b: Transantarctic Mountains + Antarctic Peninsula

Section 1: Bedrock topography

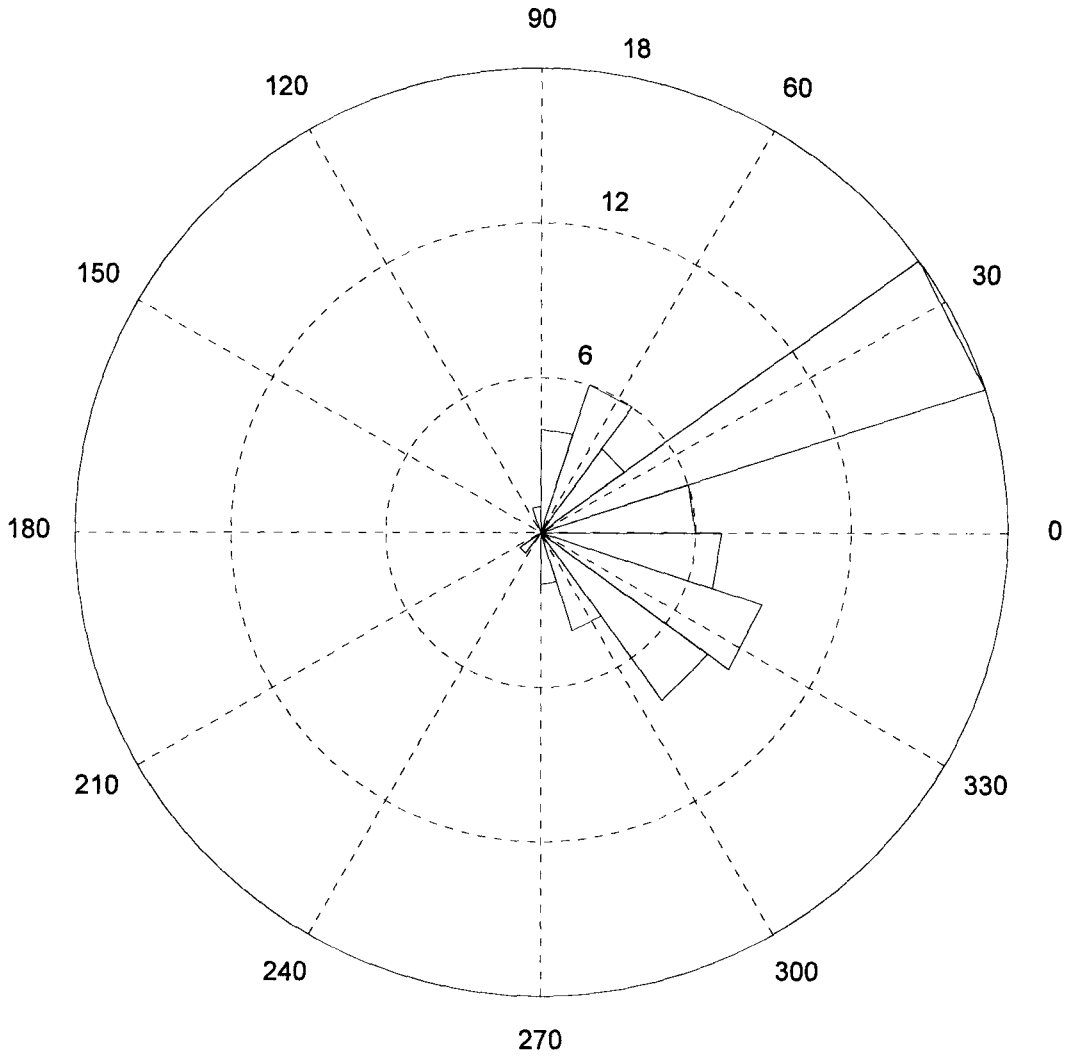

Figure c: 1st Quadrant

Section 1: Bedrock topography

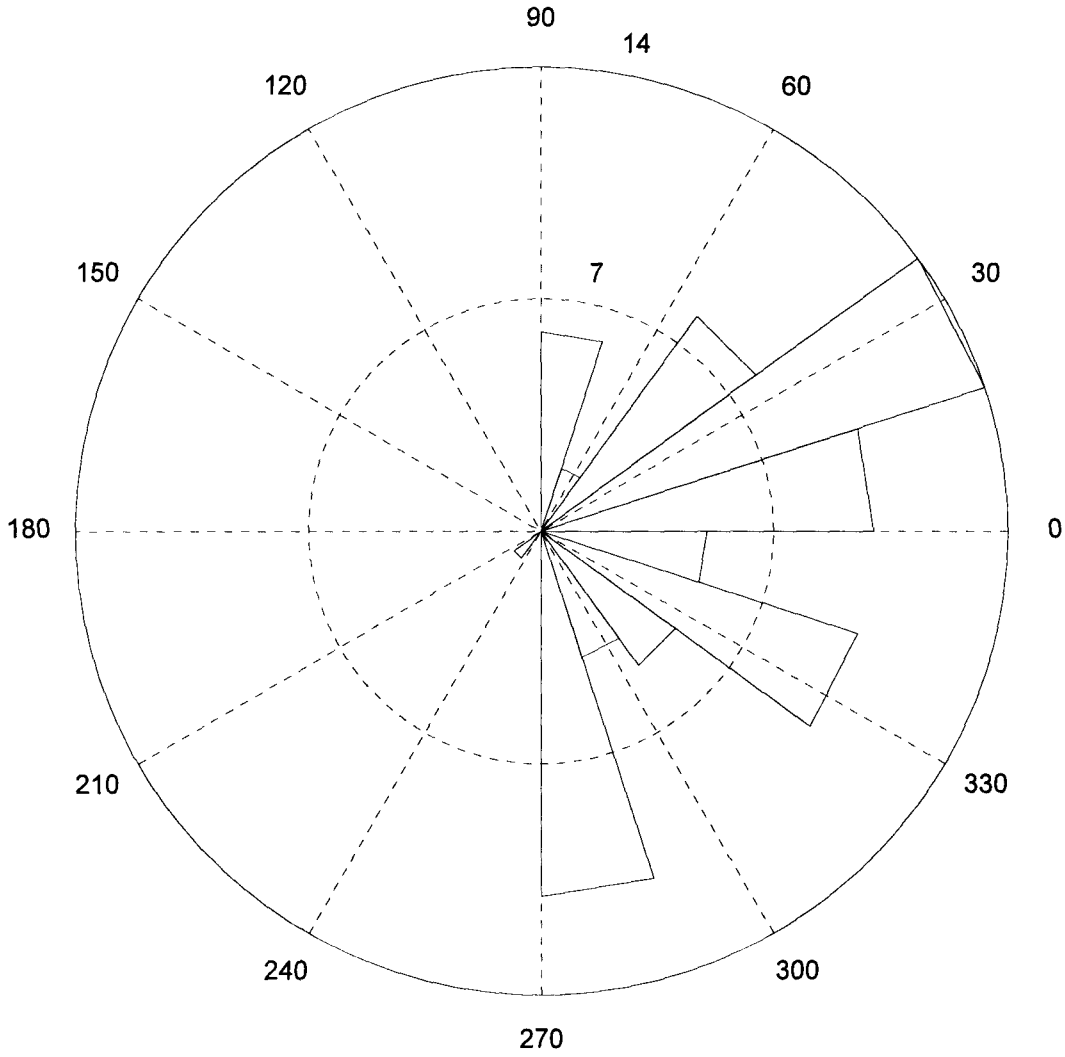

Figure d: 2nd Quadrant

Section 1: Bedrock topography

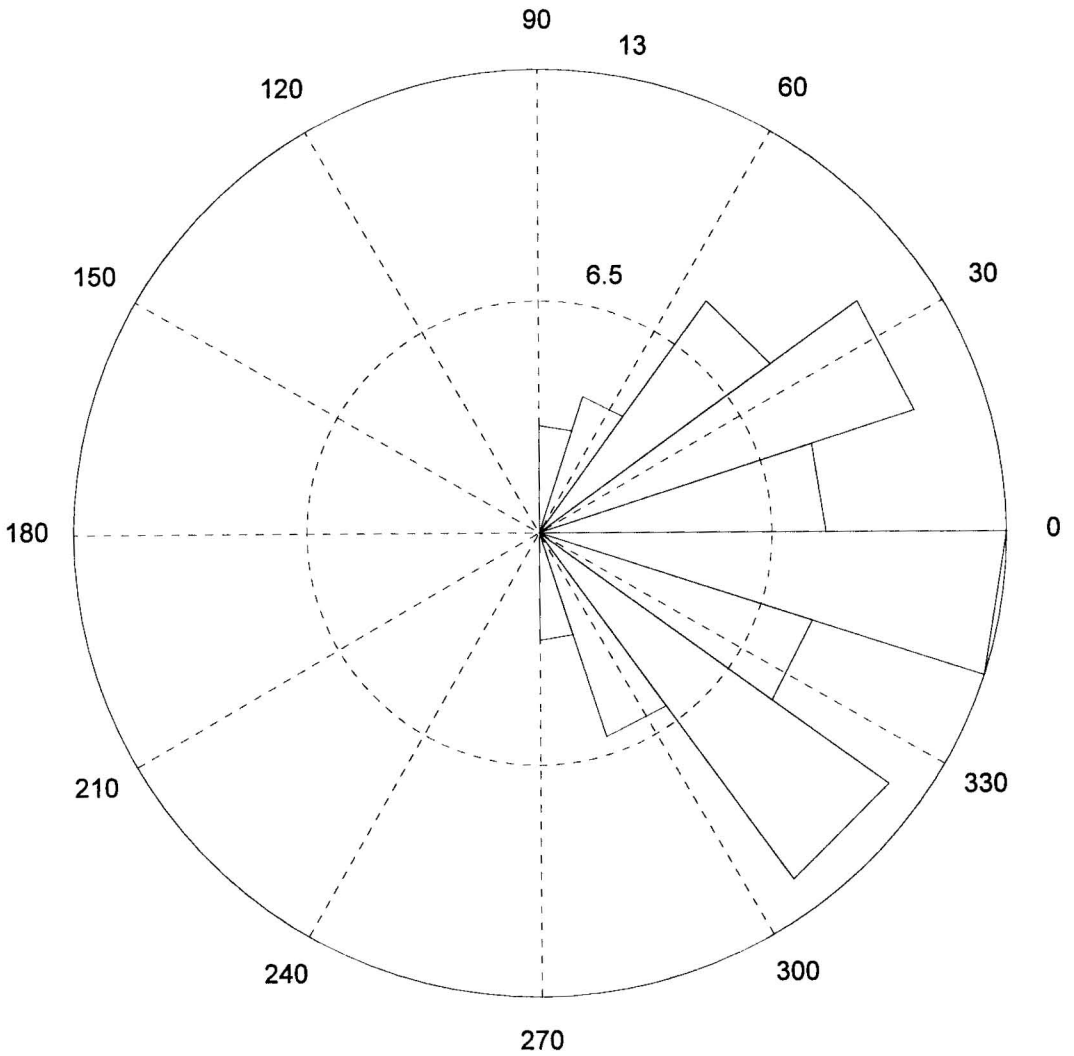

Figure e: 3rd Quadrant

Section 1: Bedrock topography

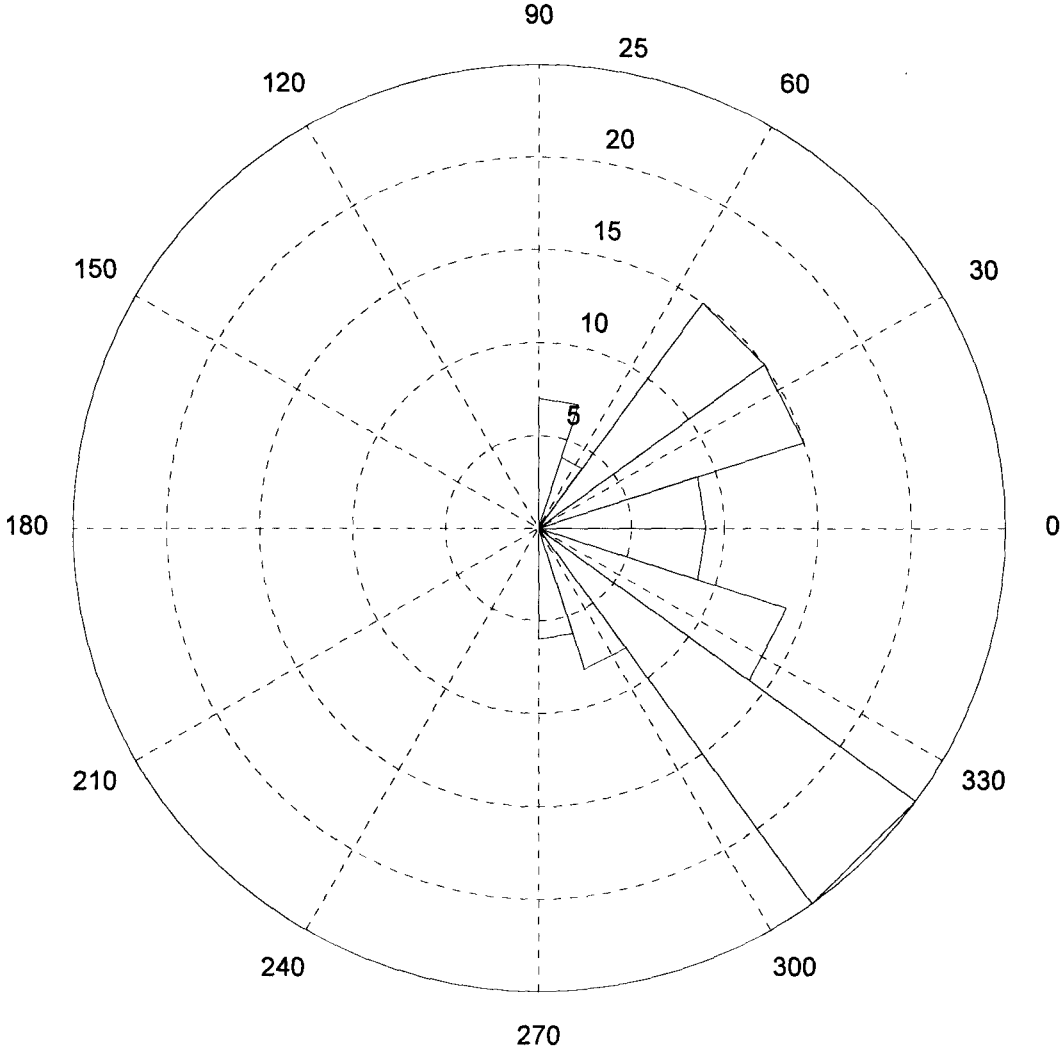

Figure f: 4th Quadrant

Section 2: NSCAT

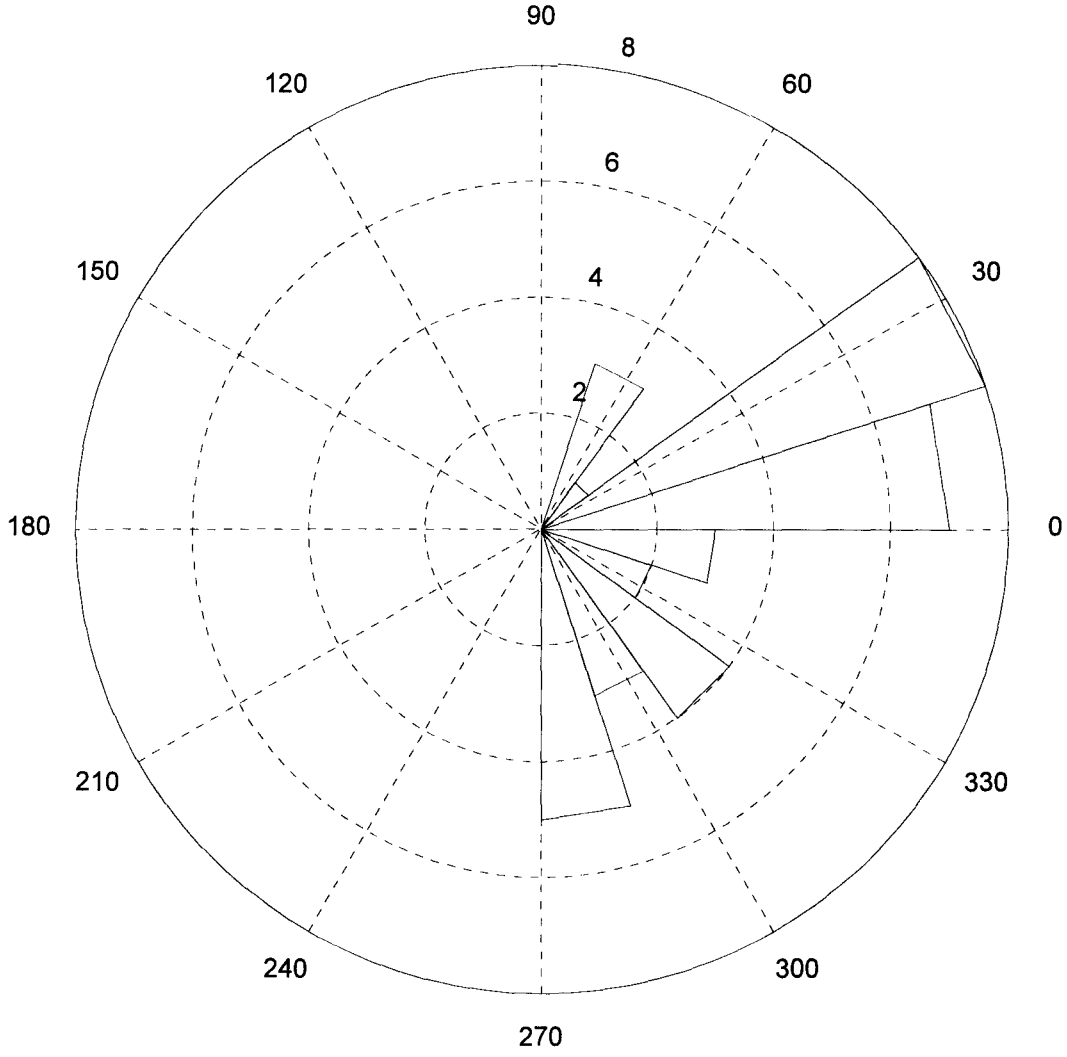

Figure a: Antarctic Peninsula

Section 2: NSCAT

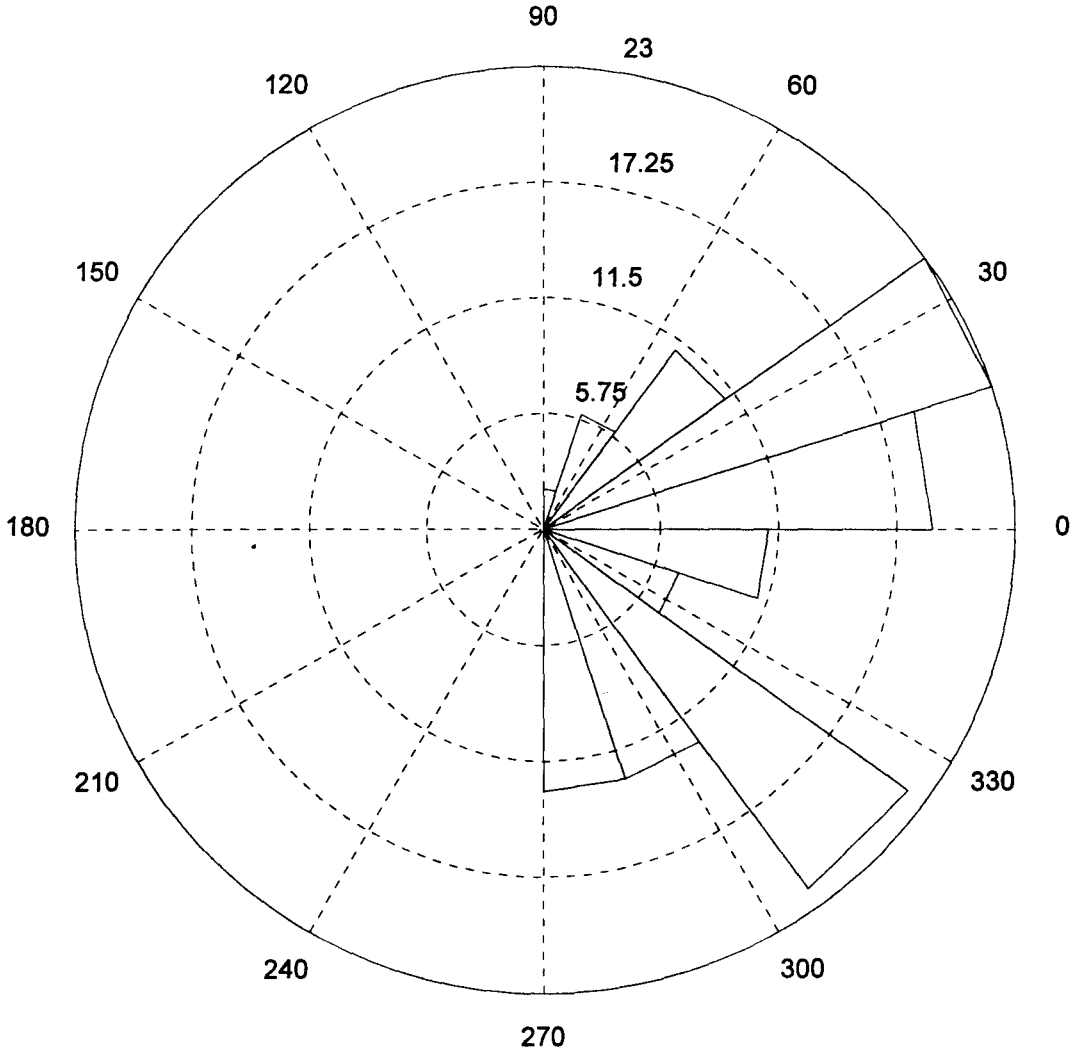

Figure b: Transantarctic Mountains + Antarctic Peninsula

Section 2: NSCAT

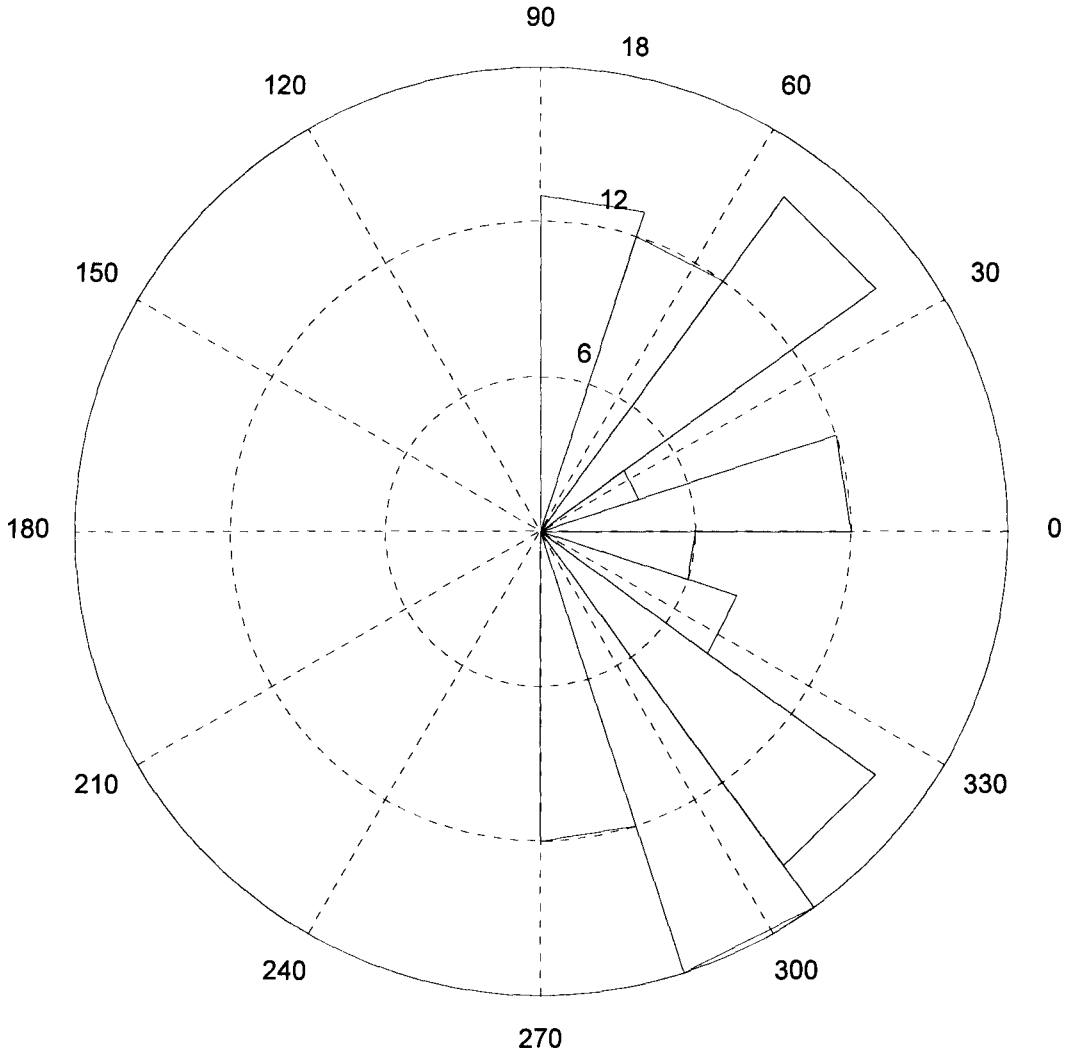

Figure c: 1st Quadrant

Section 2: NSCAT

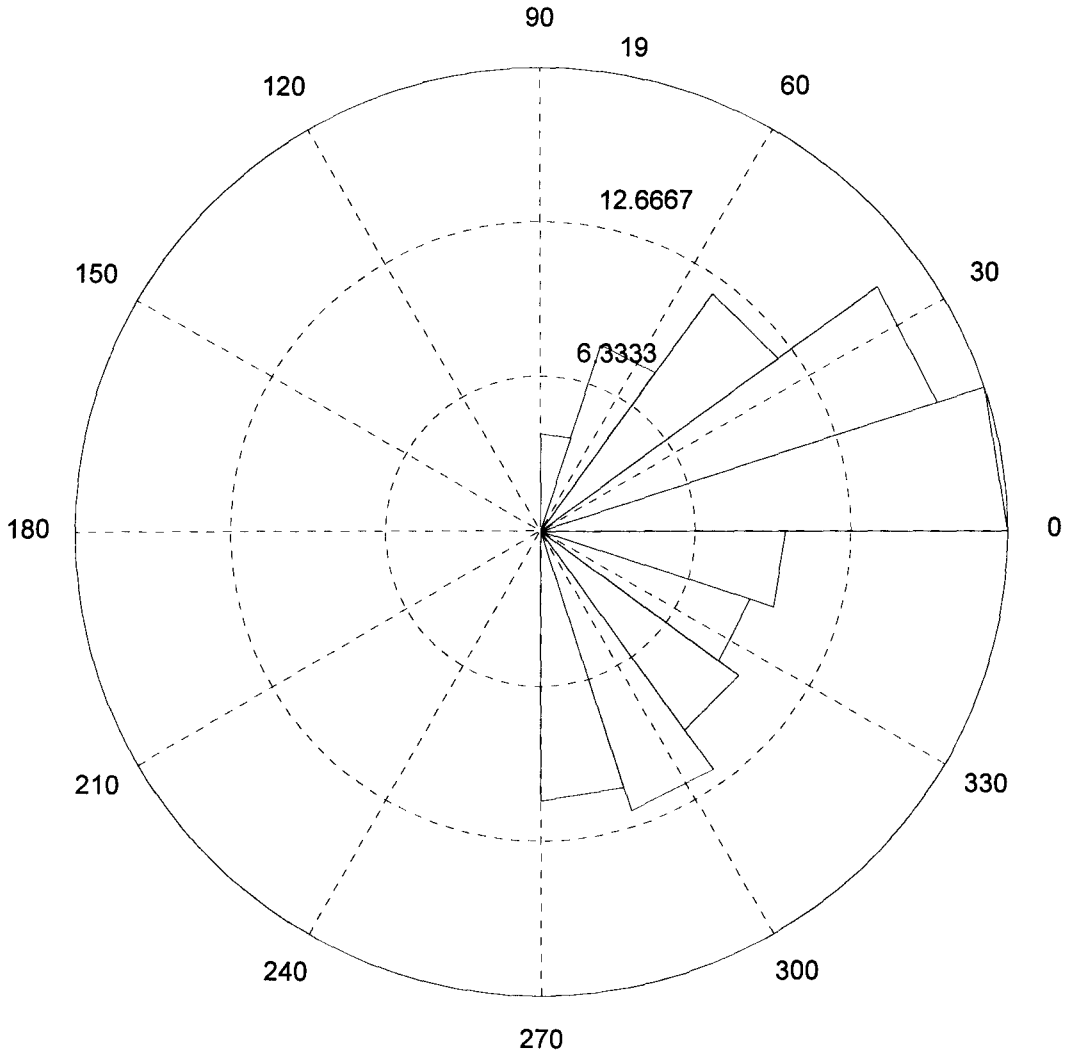

Figure d: 2nd Quadrant

Section 2: NSCAT

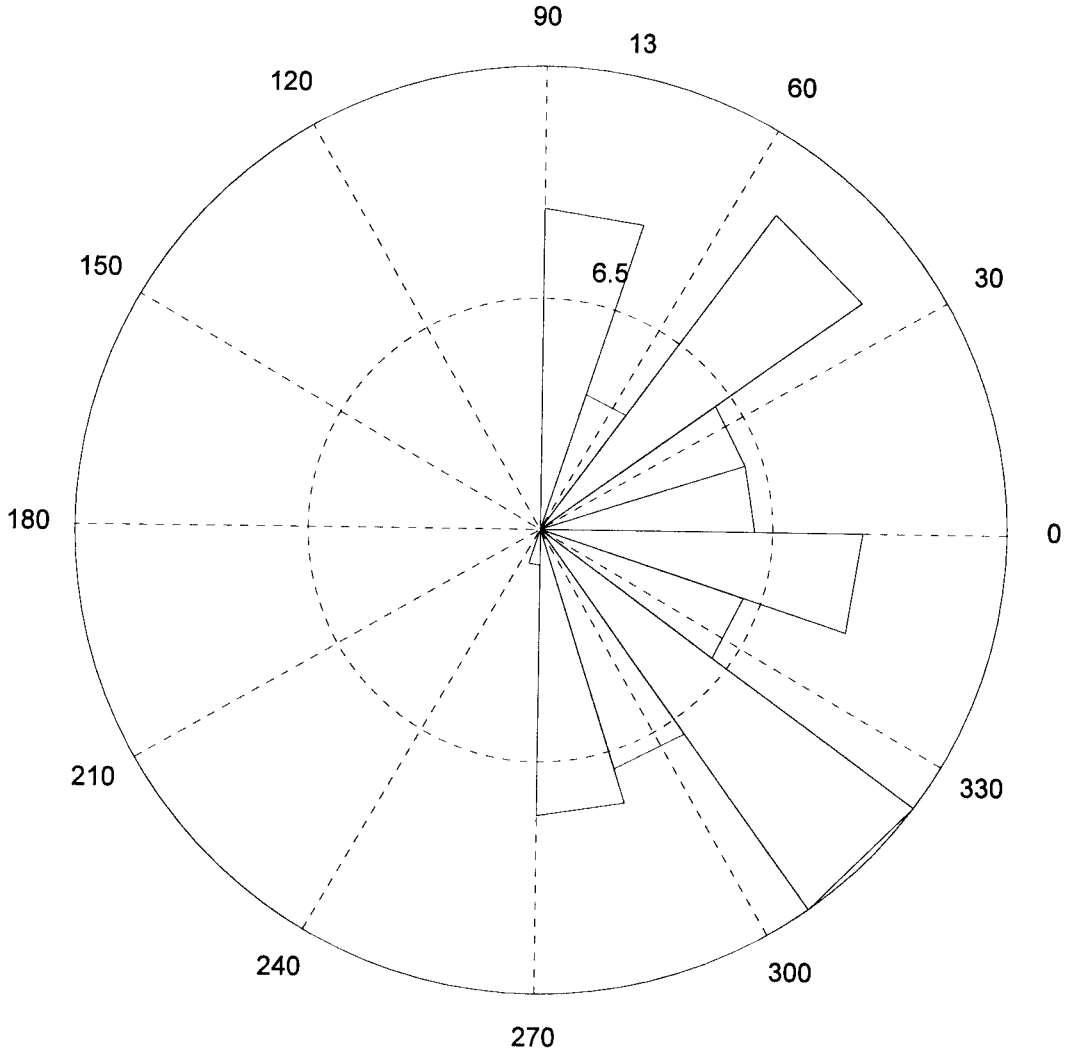

Figure e: 3rd Quadrant

Section 2: NSCAT

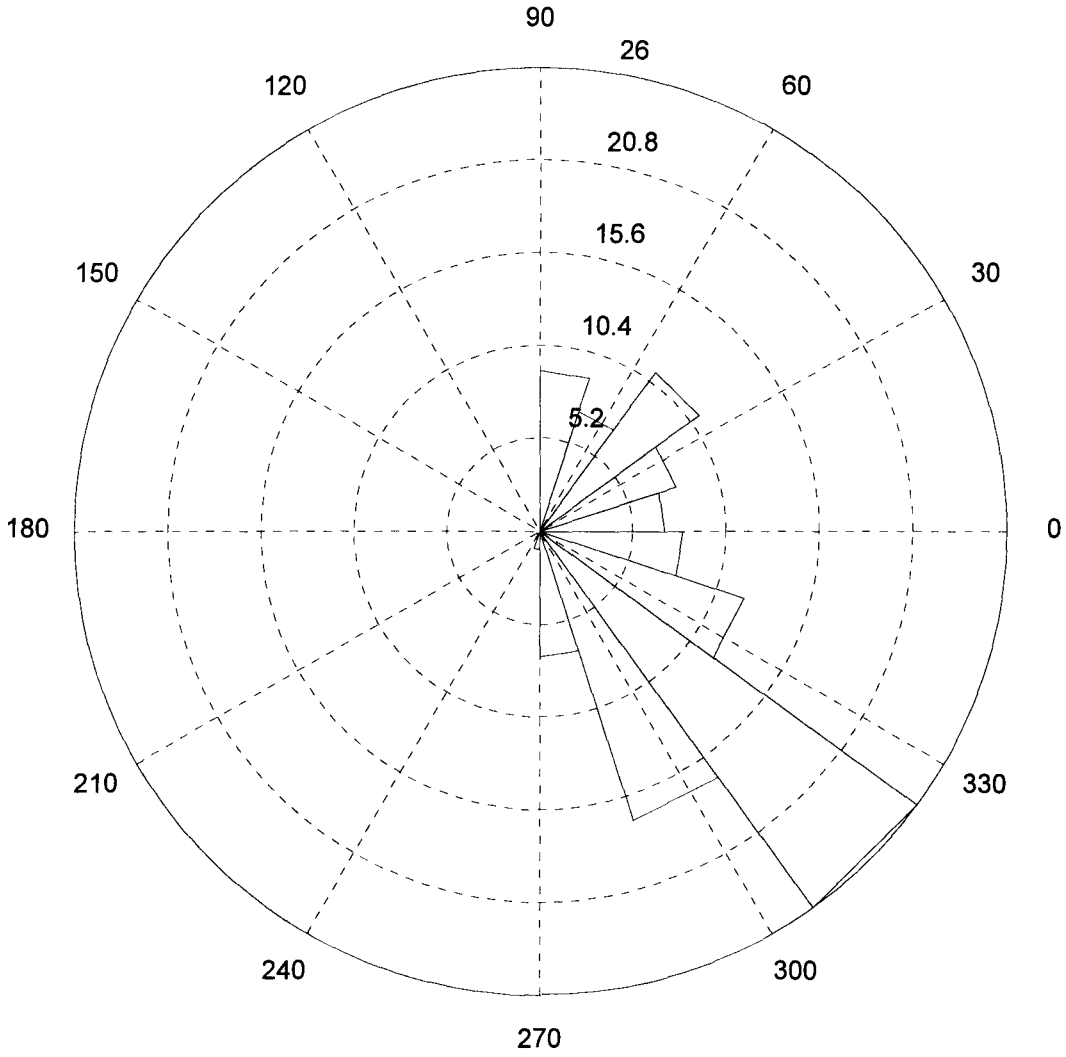

Figure f: 4th Quadrant